Axial Active Magnetic Bearing with Laminated Stators and Slit Rotor Disc Used in On-board Machinery

Sadjad Madanzadeh
Dept. of Electrical Eng.
LUT University
Lappeenranta, Finland
Sadjad.Madanzadeh@lut.fi

Kristóf Márton Szombati
Dept. of Mechanical Eng.
LUT University
Lappeenranta, Finland
Kristof.Szombati@lut.fi

Juuso Narsakka
Dept. of Mechanical Eng.
LUT University
Lappeenranta, Finland
Juuso.Narsakka@lut.fi

Tuhin Choudhury
Dept. of Mechanical Eng.
LUT University
Lappeenranta, Finland
Tuhin.Choudhury@lut.fi

Jussi Sopanen
Dept. of Mechanical Eng.
LUT University
Lappeenranta, Finland
Jussi.Sopanen@lut.fi

Tuomo Lindh
Dept. of Electrical Eng.
LUT University
Lappeenranta, Finland
Tuomo.Lindh@lut.fi

Juha Pyrhönen
Dept. of Electrical Eng.
LUT University
Lappeenranta, Finland
Juha.Pyrhonen@lut.fi

Niko Nevaranta
Dept. of Electrical Eng.
LUT University
Lappeenranta, Finland
Niko.Nevaranta@lut.fi

***Abstract*—The integration of rotating machinery with active magnetic bearings (AMBs) has been increasing, driven by the trend towards enhancing efficiency and increasing energy density through high-speed technologies. In addition, high-speed machines are being applied in increasingly demanding environments, such as on-board ships, where the entire rotating system is subject to various movements and vibrations caused by the moving platform. Such environments impose much stricter requirements on the dynamic performance of the AMB system compared to stationary systems. During dynamic operation, axial AMBs with solid iron stators and solid disc face excessive eddy current losses and temperature rise, which limits their bandwidth and dynamic response during critical events like compressor surges and thrust disturbances. The solid cores experience high eddy currents during transients, restricting the build-up or removal of flux, thereby reducing the achievable force. To overcome these limitations, this paper proposes novel configurations featuring laminated or layered stator cores and slit rotor disc, designed to reduce eddy current losses, improve thermal management, and enhance bandwidth.**

***Index Terms*—Axial active magnetic bearing, on-board rotor, suspension force, eddy current, laminated stator, slit rotor disc.**

I. Introduction

In standard industrial setups, rotating machinery is typically mounted on stationary foundations with predictable dynamics, simplifying design integration. However, many applications involve machinery subjected to base motions from external excitations, such as ship and aircraft maneuvers, vehicle bounce from road irregularities, or seismic activity. These are referred to as on-board rotor systems. When supported by AMBs, these systems must withstand dynamic, gyroscopic, and inertial loads from such disturbances. The ISO 14839 series provides general evaluation guidelines for magnetic bearing-suspended machinery. However, for marine applications, additional standards from organizations such as the International Maritime Organization (IMO) and DNV GL must also be followed [1], [2]. These standards address ship maneuverability and safety, which are crucial when designing on-board magnetic levitation systems. Ship motion during maneuvers is transmitted to the AMB stator, introducing parametric excitation that can lead to excessive vibrations and potential failure. Therefore, it is crucial to analyze the impact of ship maneuvers on AMB performance during the design of marine rotor systems.

Several studies have explored rotor dynamics under base motion, namely, [3]–[5] analyzed vibration control and stability of rotor systems subjected to base disturbances using varied modeling and validation approaches. Base excitation effects were further examined in [6], [7], revealing nonlinear behaviors such as jumps and multi-valued responses. In addition, [8]–[11] studied base motion effects on various rotor types. Similarly, periodic base motion impacts on geared and planetary systems were investigated in [12], [13]. However, these studies primarily consider simplified or specific base motion scenarios, and vibration control under complex base motions remains unaddressed. Moreover, the assumption of simple periodic motion does not reflect real-world ship maneuvers. Motivated by these gaps, [14] investigated active vibration control for base-excited rotors using a basic proportional-derivative control law, while [15] examined the performance of an AMB supporting a marine rotor system under ship maneuvers. The simulations in [15] reveal that ship-induced vibrations are more significant than those caused by rotor unbalance.

When considering the closed-loop performance of AMBs,

This research was supported by the European Commission through the project 'Efficient Zero-Emissions Gas Turbine POWER System for MARitime Transport (MARPOWER)' and the Research Council of Finland's Centre of Excellence in High-Speed Energy Conversion Systems.

they are constrained by the force capacity, linearity, and bandwidth of electromagnetic actuators, as well as limitations in feedback sensors, drivers, delays, and the control algorithm [16]. Traditional axial AMBs with solid steel stators and rotor discs face significant challenges, including elevated eddy current losses, slow force response, and temperature rise during operation [17]. The solid cores experience high eddy currents during transients, which restrict the build-up or removal of flux, consequently reducing force and degrading the bandwidth of AMBs.

The alternative axial bearing design approaches involves segmenting the thrust-bearing stator or making slits in the solid steel to shorten the eddy current paths, thereby reducing eddy current losses and enhancing dynamic performance. Studies such as [18]–[20] have investigated and modeled both solid and segmented/slit stator core AMBs and thereby improve the bandwidth of the actuator. Moreover, in [19] the development and validation of analytical models for such actuators is discussed. Another approach to reducing eddy current losses is axial AMBs with modular configurations to enable the use of laminated steel in the stators [21]. Modular designs aim to reduce eddy currents within the stator modules; however, careful design considerations are necessary. If not properly addressed, modularity can lead to a non-uniform stator structure, resulting in variations in magnetic flux density across the rotor disc. This, in turn, may introduce eddy current losses in the disc, even under steady-state conditions. Such effects become more pronounced at higher rotational speeds, suggesting that eddy current losses may still remain a challenge. Furthermore, some modular configurations may not utilize the available space efficiently for the pole area, potentially limiting the achievable force density.

This paper explores novel axial AMB configurations by analyzing and comparing designs with laminated or layered stators and slit rotor disc, while also addressing additional force requirements caused by ship movement—an aspect not extensively discussed in the literature. The only study that addresses this topic [15] proposes increasing the number of AMB coil turns and enlarging the pole area to achieve a robust solution for AMB systems in marine environments, but it does not take practical design considerations into account. The proposed laminated/layered stator configurations employ segmented or slit designs. In particular, radial lamination is introduced to improve the bandwidth of segmented/slit stator configurations, and the motivation and core idea behind combining lamination and segmentation is discussed in Section II-B. Consequently, lamination is not an alternative to segmentation/slits in stator but rather an approach that further enhances its effectiveness. This paper is organized as follows. Section II defines the problem describes its various aspects and introduces a novel axial AMB design technology. In Section III, the operational principle of the axial AMB is presented. Section IV presents analyses and discussions to validate the proposed concept. Finally, the conclusions are drawn in Section V.

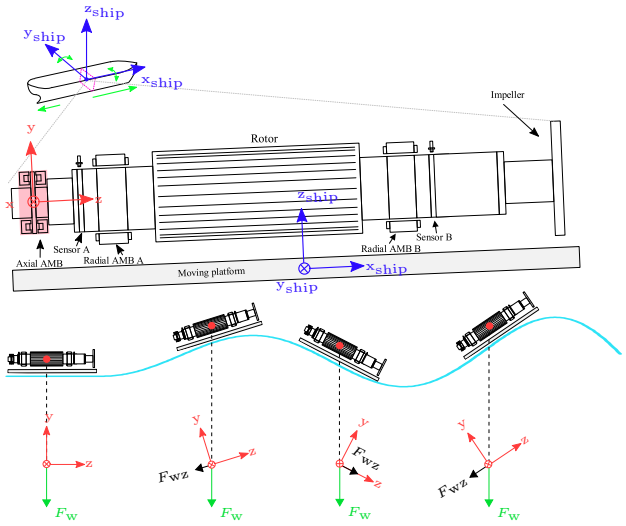

Fig. 1. Illustration of an active magnetic bearing-suspended rotor system in marine applications, showing both radial and axial suspension (above), and the effect of the pitching motion on the force applied to the axial AMB (below).

II. Problem Statement and Proposed Technology

The principle of an on-board AMB-suspended rotor system for marine applications is illustrated in Fig. 1. Similar to traditional high-speed rotor setups, it employs two radial AMBs and a U-shaped axial AMB to stabilize the rotor. Operating under dynamic ship movements and base excitations [15], the axial AMB must adapt to varying loads influenced by these motions and external factors like changing marine conditions. As an illustrative example, Fig. 1 demonstrates how the rotation of the ship about its transversal axis (pitch) influences the axial AMB load due to the rotor weight (F_{w}). Additionally, the axial AMB must counteract forces during operation, start-up, and shutdown, including compressor thrust, electromagnetic imbalances, inertial forces from acceleration, fluid pressure variations, rotor misalignment, thermal expansion, and external vibrations. These combined forces create the total axial load, which the AMB stabilizes to maintain smooth motor/generator performance.

A. Forces Induced by Ship Motions on Axial AMB

As Fig. 1 shows, in ship motion analysis, the $\mathrm{x_{ship}}$-axis runs longitudinally from bow to stern, the $\mathrm{y_{ship}}$-axis extends laterally from port to starboard, and the $\mathrm{z_{ship}}$-axis is vertical from hull to deck. Translational motions along these axes include surge ($\mathrm{x_{ship}}$), sway ($\mathrm{y_{ship}}$), and heave ($\mathrm{z_{ship}}$), while rotational motions include roll (around $\mathrm{x_{ship}}$), pitch (around $\mathrm{y_{ship}}$), and yaw (around $\mathrm{z_{ship}}$). These axes and motions are essential for analyzing dynamic forces affecting axial AMBs in marine environments. The total axial bearing force considering only the pitch and roll motions of the vessel and gravity can be expressed as

$$F_{\mathrm{axial}} = m\left(\ddot{\alpha} r_{\mathrm{xz,ship}} \sin\phi + \dot{\alpha}^2 r_{\mathrm{xz,ship}} \cos\phi - \mathrm{g}\sin\alpha\right), \tag{1}$$

TABLE I
PERMISSIBLE MOTIONS IN SHIPS (LENGTH $\geq$ 100 m) APPLICABLE TO ONBAORD TURBOMACHINERY COMPONENTS [22]

Rotational motion		**Angle of inclination** [deg]	
		Static	**Dynamic (time period [s])**
Fore-and-aft (pitch)		5	7.5 (5)
Athwartship (roll)		15	25 (10)
Translational motion		**Acceleration** [$\frac{\text{m}}{\text{s}^2}$]	
Forward direction		0.25 g	
Aft direction		0.5 g	

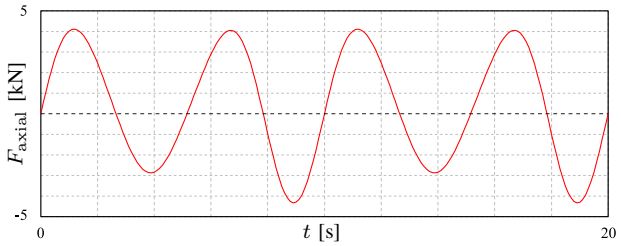

Fig. 2. Analyzed axial bearing force during combined pitch and roll motion.

where, for the case studied, $m = 576.4\,\text{kg}$ is the mass of the rotor, α is the pitch angle of the vessel, $r_{\text{xz,ship}} = \sqrt{x_{\text{ship}}^2 + z_{\text{ship}}^2}$ is the projection of the distance of the center of inertia (CoI) of the rotor expressed in the frame of reference of the vessel to the x_{ship}-z_{ship} plane, $x_{\text{ship}} = -51.19\,\text{m}$ is the longitudinal position of the CoI of the rotor expressed in the frame of reference of the vessel, $z_{\text{ship}} = 26.47\,\text{m}$ is the vertical position of the CoI of the rotor expressed in the frame of reference of the vessel, $\phi = \tan^{-1}(\frac{z_{\text{ship}}}{x_{\text{ship}}})$ and $g = 9.81\,\text{ms}^{-2}$ is the gravity constant. It is worth noting that the velocity and accelerations in the vertical direction are so small, that they can be ignored.

Table I outlines the ship motions to be considered based on international standards, for example [22], while Fig. 2 presents the analysis of axial AMB force induced by only the pitch and roll motions within the limits set by this standard. In the example rotor configuration considered here, the maximum axial force amplitude due to these loads is 4329 N. This means that the design of the axial bearing needs to ensure sufficient force capacity to handle these loads without reaching magnetic saturation or exceeding the current and voltage limits of the amplifier. The axial AMB considered in this paper is designed to have a total maximum capacity of 15.75 kN, defined by the process-related forces and operational constraints to ensure stable performance of the conceptual turbine-compressor, where the dimensions of the axial AMB with a solid stator and rotor were optimized through an analytical optimization process.

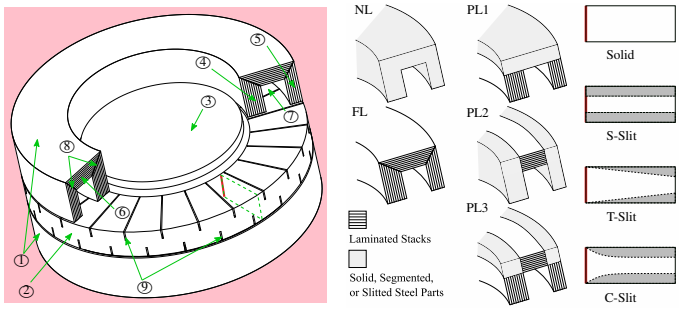

(a) (b)

Fig. 3. Proposed configurations of axial AMB: (a) U-shaped axial magnetic bearing with laminated stators and slit rotor disc: ① stator with a laminated core, which can be in segmented form or include slits, ② slit rotor disc, ③ rotor shaft, ④ inner pole with rolled lamination stacks, ⑤ outer pole with rolled lamination stacks, ⑥ yoke with lamination stacks, ⑦ stator slot, ⑧ angled cut in lamination stacks, ⑨ slit, and (b) Cross-sectional views of the four designs of the rotor disc (Solid, S-Slit, T-Slit, C-Slit) and five stator core configurations (conventional non-laminated (NL), fully laminated (FL), partially laminated Type 1 (PL1), partially laminated type 2 (PL2), partially laminated type 3 (PL3)).

B. Configurations with Laminated/Layered Stators and Slit Rotor Disc

To reduce eddy current losses and enhance the dynamic performance of the axial AMB, this paper analyzes some possible innovative design configurations and existing structures as summarized in Fig. 3. The solution features laminated stators and a slit rotor disc design to reduce eddy currents. Fig. 3 (b) illustrates various stator configurations, including fully laminated (FL), partially laminated (PL) with a solid yoke, solid poles, or joints connecting laminated poles to the yoke. It should be mentioned that the solid parts in these novel laminated configurations and the conventional non-laminated (NL) structure can be segmented or slit to reduce the eddy current in these parts. Rotor disc designs include solid disc, slit disc (SD) with straight (S) slits, triangular (T) slits, and curved (C) slits, with the C-type slit identified as optimal for its reduced mechanical stress.

In this paper, a laminated/layered design is introduced as an enhancement to segmented/slit stator designs. Specifically, segmented fully laminated/layered (SFL) and segmented partially laminated/layered (SPL) configurations are presented to effectively reduce eddy currents, thereby further improving the bandwidth of the actuator. As demonstrated by analyses in Section IV, incorporating SD into the configuration can yield additional performance improvements.

To illustrate the principle behind introducing radial laminations/layers into the segmented/slit stator configuration—resulting in segmented laminated/layered (SL) designs, Fig. 4 uses the components of the current density vector $\vec{J}$ in the cylindrical coordinate system. In this figure, the eddy current distribution and the effect of the lamination are illustrated using partial models of axial AMBs. It is worth noting that, for simplicity, the term "laminated" is used throughout the paper to refer to both laminated and layered structures. This figure shows that in the NL configuration, the

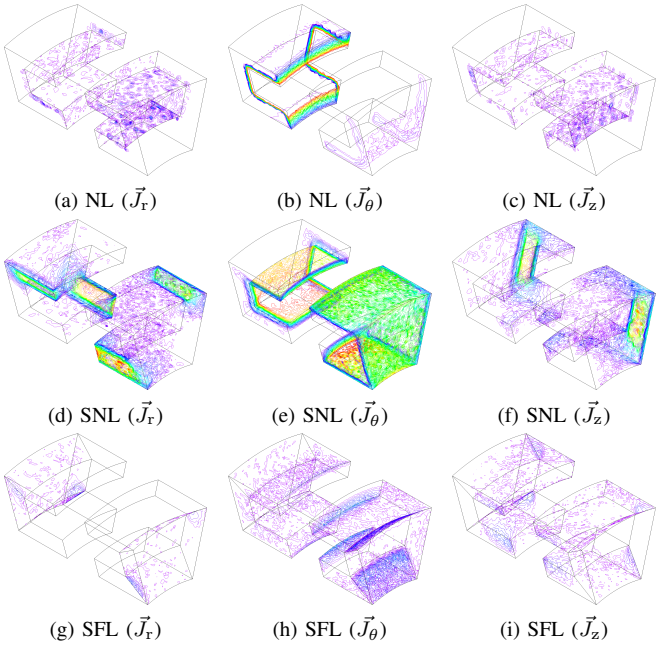

(a) NL ($\vec{J}_\mathrm{r}$) (b) NL ($\vec{J}_\theta$) (c) NL ($\vec{J}_\mathrm{z}$)

(d) SNL ($\vec{J}_\mathrm{r}$) (e) SNL ($\vec{J}_\theta$) (f) SNL ($\vec{J}_\mathrm{z}$)

(g) SFL ($\vec{J}_\mathrm{r}$) (h) SFL ($\vec{J}_\theta$) (i) SFL ($\vec{J}_\mathrm{z}$)

Fig. 4. Eddy current distribution in the radial, circumferential, and axial directions for a partial model of the NL configuration, as well as a single segment from the SNL and SFL configurations.

dominant component is $\vec{J}_\theta$, indicating that the most effective strategy for reducing eddy currents in this case is to interrupt their path in the θ-direction using segments or slits. A single segment of the segmented non-laminated (SNL) configuration is depicted in Fig. 4d to Fig. 4f. It is evident that in the SNL structure, the eddy current paths differ from those in the NL configuration, introducing radial and axial components in addition to the circumferential one. Therefore, to further suppress these currents, radial laminations were introduced, limiting the eddy current paths in the SNL configuration. As shown in Fig. 4g to Fig. 4i, radial lamination/layers significantly impact the eddy current distribution, resulting in a significant reduction in eddy current loss and, consequently, an improvement in the dynamic performance and bandwidth of the axial AMB.

Electric machines and radial AMBs commonly use laminated stators to minimize eddy current losses and improve efficiency. However, laminated stators in axial AMBs present several limitations and challenges. One major drawback is the reduced structural rigidity of laminated stators compared to solid-core designs, which may compromise the mechanical stability required for high-precision AMBs. This limitation is further compounded by difficulties in connecting stator parts and ensuring the strength of the connecting mechanism against axial forces. Additionally, the presence of insulation layers between laminations increases magnetic reluctance, potentially weakening the magnetic flux and reducing overall bearing performance. Vibrations and dynamic loads in axial AMBs may also contribute to the degradation of laminations over time, affecting long-term reliability. The manufacturing process of laminated stators further adds complexity, for example, due to the need for precise angled cuts in laminations and the challenge of forming cylindrical lamination stacks. These factors increase fabrication difficulty and cost. Given these considerations, the suitability of laminated stators for axial magnetic bearing applications must be carefully evaluated based on specific operational requirements. Assembly and fixation of components is also one of the primary challenges in the segmented laminated axial AMB structure. Figure 5 presents several representative methods proposed for connecting and assembling the components of the AMB.

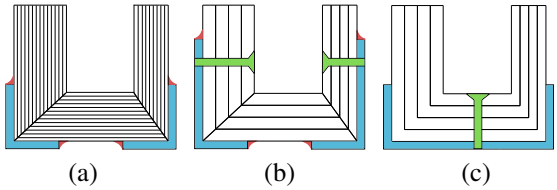

(a) (b) (c)

Fig. 5. Exemplary methods for assembling and securing an axial AMB using soldering and screwing: (a) Laminated stator with components connected by soldering. (b) Layered stator with components secured by a combination of soldering and screwing. (c) Layered stator constructed from U-shaped layers, each made from solid steel—for example, through machining or other suitable manufacturing processes—and secured together by screwing.

III. Principle of Axial Active Magnetic Bearings

An axial active magnetic bearing generates bidirectional forces along its symmetry axis through opposing electromagnets. Each electromagnet acts as a stator, with a coil placed between two poles, producing an attractive force on the rotor disc.

A. Force Capacity

The magnetic force in the axial AMB system is derived from the partial derivative of magnetic co-energy with respect to the displacement z, given by $F_\mathrm{z} = \frac{B^2 A_\mathrm{p}}{\mu_0}$ where μ_0 is the permeability of air, A_p is the pole area, and the magnetic flux density B at the air gap is given by $B = \mu_0 \frac{Ni}{2z_0}$, based on Ampere's law. This expression assumes negligible flux leakage and no magnetic reluctance in the steel parts of the actuator. However, this simplification can lead to overly optimistic results, particularly when eddy currents obstruct the flux flow within the circuit. Here, N is the number of coil turns, and i is the current. Substituting this into the force equation, the magnetic force is obtained as $F_\mathrm{z} = \frac{L^2 i^2}{\mu_0 N^2 A_\mathrm{p}}$ where $L = \frac{N^2}{2\mathcal{R}}$ is the inductance, and $\mathcal{R} = \frac{z_0}{\mu_0 A_\mathrm{p}}$ represents the air-gap reluctance. In steady-state conditions, the actual reluctance is slightly higher than predicted by this equation. When eddy currents are present, the apparent reluctance increases significantly compared to this idealized value.

For opposing electromagnets, the coil currents are defined as i_r and $i_\mathrm{l} = i_\mathrm{b} \pm i_\mathrm{c}$ for the right and left stators, respectively, where i_b represents the bias current and i_c the control current. The air gaps are z_r and $z_\mathrm{l} = z_0 \mp z$, with z_0 as the nominal air gap and z as the rotor displacement. Positive displacement z corresponds to a shift to the right, while negative z indicates

a shift to the left. The resulting force is thus a function of the rotor displacement and the control current as

$$F_{\mathrm{z}} = \frac{\mu_0 N^2 A_{\mathrm{p}}}{4}\left[\frac{(i_{\mathrm{b}}+i_{\mathrm{c}})^2}{(z_0-z)^2} - \frac{(i_{\mathrm{b}}-i_{\mathrm{c}})^2}{(z_0+z)^2}\right]. \tag{2}$$

In the linear operating area, (2) can be approximated as $F_{\mathrm{z}} = k_{\mathrm{i}} i_{\mathrm{c}} + k_{\mathrm{z}} z$ where the current and position stiffness coefficients are given by $k_{\mathrm{i}} = \frac{\mu_0 N^2 A_{\mathrm{p}} i_{\mathrm{b}}}{z_0^2}$ and $k_{\mathrm{z}} = \frac{\mu_0 N^2 A_{\mathrm{p}} i_{\mathrm{b}}^2}{z_0^3}$, respectively.

B. Bandwidth

In an axial AMB system, the bandwidth $f_{-3\,\mathrm{dB}}$, is derived from the frequency response of the open-loop transfer function. It is typically defined as the frequency at which the gain decreases to $\frac{\sqrt{2}}{2}$ of its DC value, corresponding to a $-3\,\mathrm{dB}$ drop. This bandwidth reflects the frequency-dependent behavior of the current-to-force and current-to-flux transfer functions, which are proportional to the inverse of the reluctance function (as described in [23]). The bandwidth can be expressed analytically as:

$$f_{-3\,\mathrm{dB}} = \delta \frac{\mathcal{R}^{0^2}}{2\pi \mathcal{C}^2} \tag{3}$$

where $\mathcal{R}^0$ is the static reluctance of the electromagnet at zero frequency, δ is a coefficient dependent on the stator structure, such as the number of segments, and $\mathcal{C}$ is a parameter governing the significance of eddy currents, with $\mathcal{C} = 0$ representing a system with no eddy current effects. This approach provides a more comprehensive representation of the frequency-dependent behavior of the system based on the reluctance function given by $\mathcal{R}(s) = \mathcal{C}\sqrt{s} + \mathcal{R}^0$ highlighting the effect of eddy currents on system dynamics. Approximate models using this formulation have been shown to closely represent the actual transfer function of magnetic suspension actuators [23].

The bandwidth defined by (3) can be calculated analytically, numerically (e.g., FEM) or experimentally. The $-3\,\mathrm{dB}$ bandwidth is critical for frequency-domain analysis and control system design, as it characterizes the ability of the system to track signals and reject disturbances.

IV. Analysis of the Designed Axial Bearings

The performance of the studied axial AMBs, with key specifications and material properties listed in Table II and Table III, respectively, was evaluated using both 2D and 3D FEM simulations (JMAG software). The analysis covers key performance aspects, including the behavior of axial AMBs under steady-state conditions at various operating points, as well as their bandwidths, as detailed in the following.

Segmentation, slits, and lamination all affect the pole area, depending on the number of segments, slits, and laminated layers, insulation portions in segmentation and lamination, and the cut gap in slits. These factors must be carefully considered based on application requirements.

To ensure a manageable number of studied cases and provide a focused comparison of eddy current losses, this study assumes that segmentation, slitting, and lamination do not reduce the pole area. As a result, segmented and slit stators are treated equivalently, assuming that their primary function is to divide the stator circumferentially. Therefore, only the segmented stator is analyzed as a representative case for both segmented and slit stators to compare with the laminated configurations proposed in this study.

A. Force Capacity

In Fig. 6a, the relationship between force amplitude and control current is shown, highlighting the force coefficient k_{i}. Similarly, Fig. 6b illustrates the force-displacement relationship, emphasizing k_{z} in the proposed design. The linearized force is represented by a blue dashed line in Fig. 6a. However, in Fig. 6b, the force remains inherently linear for a 1 mm air gap but may exhibit nonlinearity when the air gap exceeds 2 mm. Furthermore, Fig. 7 illustrates AMB performance across operating points as a function of displacement and control current, showing (a) bearing force and (b) inductance. The contour plots reveal the nonlinear characteristics of the system, depicting how force generation and inductance vary with displacement and control current. These nonlinearities help define the admissible operating range of the AMB system in marine applications, a topic that requires further evaluation as highlighted in [24].

B. Bandwidth

To verify the performance of the magnetic bearing for marine applications, where dynamic forces result from ship movement, a frequency analysis was performed using 3D finite element analysis applying current perturbations at 3, 6, 12, 25, 50, 100, and 190 Hz with bias and peak current values specified in Table II. In the segmented stator configuration, the stator comprises 12 segments, matching the 12 slits on each side of the slit rotor disc, where the depth of each slit is one-third of the disc thickness. The normalized magnitudes of the force for different topologies are shown in Fig. 8, and the corresponding bandwidths $f_{-3\,\mathrm{dB}}$, described in Subsection III-B, are summarized in Table IV. Considering the results presented in Fig. 8 and Table IV, along with the MW-size machine considered for large vessels and the ship motion

TABLE II
Specifications of the Studied AMBs

Parameter (Symbol, Unit)	Value
Peak voltage (V_{peak}, V)	92
DC link voltage (V_{dc}, V)	230
Peak current (I_{peak}, A)	16
Peak force (F_{peak}, kN)	15.75
Bias current (I_{bias}, A)	8
Coil resistance (R, Ω)	0.57
Coil inductance (L, H)	0.28
Number of turns (N, turns)	188
Current stiffness coefficient (k_{i}, N/A)	3094
Position stiffness coefficient (k_{z}, N/mm)	24877
Rotational speed (ω_{m}, rpm)	12000

TABLE III
MECHANICAL PROPERTIES OF S355 MATERIAL

Parameter (Symbol, Unit)	**S355**
B knee point (B_{knee}, T)	1.3
H knee point (H_{B}, A/m)	1500
Young's modulus (E, GPa)	210
Poisson's ratio (ν)	0.3
Density (ρ, kg/m^3)	7800
Yield strength (σ, MPa)	355
Tensile strength (UTS, MPa)	550
Thermal expansion coefficient (α_{T}, $\times 10^{-6}$/K)	12.0

Note: In its laminated form, S355 sheets have a thickness of 1 mm.

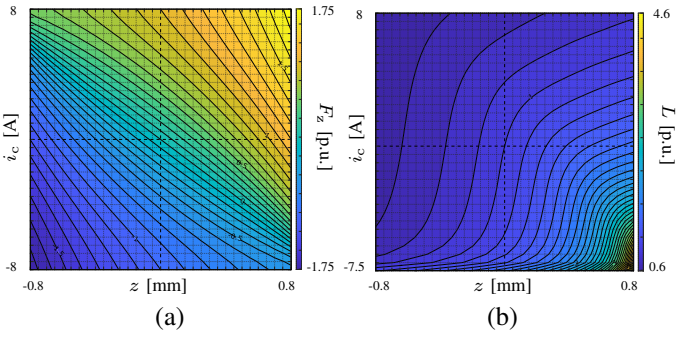

Fig. 7. AMBs performance across operating points as a function of displacement and control current: (a) bearing force, (b) inductance.

criteria outlined in Table I, the NL structure demonstrates the potential to meet the dynamic performance requirements for such applications. Similarly, the NL+SD configuration offers performance close to this level. For applications demanding higher bandwidth, the SNL or SNF configurations can provide a significant enhancement in bandwidth, which could be further enhanced when combined with SD. For example, higher bandwidth may be justified under specific conditions to withstand extreme marine environments—such as base excitations, varying vessel sizes, or vertical/horizontal rotor configurations.

V. CONCLUSION

This paper investigates the design and performance improvements of axial AMBs through the proposal and analysis of various configurations featuring laminated stators and slit rotor disc. These novel configurations aim to enhance dynamic response and address critical challenges associated with traditional AMBs, such as eddy current losses and bandwidth limitations, particularly relevant in demanding, high-speed

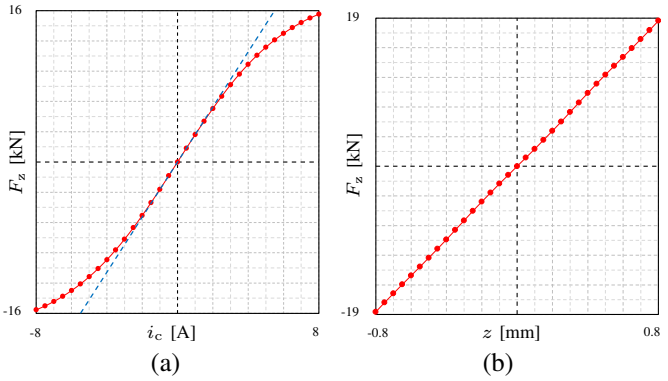

Fig. 6. AMBs performance: (a) Force vs. control current, (b) Force vs. rotor displacement.

TABLE IV
SUMMARY OF BANDWIDTH VALUES OBTAINED FROM THE FREQUENCY ANALYSIS (FIG. 8)

Configuration	NL	NL+SD	SNL	SNL+SD	SFL	SFL+SD
$f_{-3\,\text{dB}}$[Hz]	15.75	17	44	52	86	125

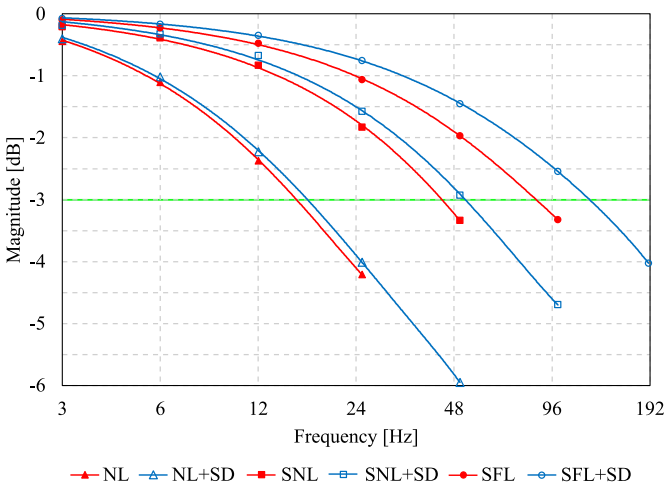

Fig. 8. Frequency response of the current-to-force transfer function for normalized force.

electric machine for marine applications. Furthermore, the study examines key manufacturing challenges and design considerations, offering practical insights into the implementation and feasibility of these configurations. The findings indicate that each proposed laminated configuration, along with existing slit and segmented designs, provides distinct advantages. Selecting the optimal configuration depends significantly on specific application requirements and operational constraints. A careful evaluation of these aspects can effectively maximize performance, efficiency, and reliability, thus supporting the broader adoption of axial AMBs in dynamic, high-speed applications.

REFERENCES

[1] International Maritime Organization, "Resolution standards for ship maneuverability," MSC.137(76), Dec. 2002.

[2] International Maritime Organization, "Explanatory notes to the standards for ship maneuverability," MSC/Circ 1053, Dec. 2002.

[3] M. O. T. Cole, P. S. Keogh, and C. R. Burrows, "Vibration control of a flexible rotor/magnetic bearing system subject to direct forcing and base motion disturbances," *Proceedings of the Institution of Mechanical Engineers, Part C: Journal of Mechanical Engineering Science*, vol. 212, no. 7, pp. 535–546, Jul. 1998.

[4] F. Lin and G. Meng, "Study on the dynamics of a rotor in a maneuvering aircraft," *ASME Journal of Vibration and Acoustics*, vol. 125, no. 3, pp. 324–327, 2003.

[5] M. Duchemin, A. Berlioz, and G. Ferraris, "Dynamic behaviour and stability of a rotor under base excitation," *ASME Journal of Vibration and Acoustics*, vol. 128, no. 5, pp. 576–585, 2006.

[6] A. S. Lee, B. O. Kim, and Y. Kim, "A finite element transient response analysis method of a rotor-bearing system to base shock excitations using the state-space newmark scheme and comparisons with experiments," *Journal of Sound and Vibration*, vol. 297, pp. 595–615, 2006.

[7] M. H. Eissa, U. H. Hegazy, and Y. A. Amer, "Dynamic behavior of an amb supported rotor subject to harmonic excitation," *Applied Mathematical Modelling*, vol. 32, no. 7, pp. 1370–1380, Jul. 2008.

[8] Q. Han and F. Chu, "Dynamic response of cracked rotor-bearing system under time-dependent base movements," *Journal of Sound and Vibration*, vol. 332, no. 25, pp. 6847–6870, Dec. 2013.

[9] M. Dakel, S. Baguet, and R. Dufour, "Nonlinear dynamics of a support-excited flexible rotor with hydrodynamic journal bearings," *Journal of Sound and Vibration*, vol. 333, pp. 2744–2799, 2014.

[10] M. Dakel, S. Baguet, and R. Dufour, "Steady-state dynamic behavior of an on-board rotor under combined base motions," *Journal of Vibration and Control*, vol. 20, no. 15, pp. 2254–2287, 2014.

[11] Y. Yi, Z. Qiu, and Q. Han, "The effect of time-periodic base angular motions upon dynamic response of asymmetric rotor system," *Advances in Mechanical Engineering*, Mar. 2018.

[12] Q. Han and F. Chu, "Dynamic behaviors of a geared rotor system under time-periodic base angular motions," *Mechanism and Machine Theory*, vol. 78, pp. 1–14, Aug. 2014.

[13] X. Qiu, Q. Han, and F. Chu, "Dynamic modeling and analysis of the planetary gear under pitching base motion," *International Journal of Mechanical Sciences*, vol. 141, pp. 31–45, Jun. 2018.

[14] A. S. Das, J. K. Dutt, and K. Ray, "Active vibration control of flexible rotors on maneuvering vehicles," *AIAA Journal*, vol. 48, no. 2, pp. 340–353, 2010.

[15] T. Soni, J. K. Dutt, and A. S. Das, "Magnetic bearings for marine rotor systems—effect of standard ship maneuver," *IEEE Transactions on Industrial Electronics*, vol. 68, no. 2, pp. 1055–1064, 2021.

[16] E. Kurvinen, R. Fittro, and E. Maslen, "Improving compressor surge performance with advanced control," *Proceedings of the Institution of Mechanical Engineers, Part I: Journal of Systems and Control Engineering*, vol. 230, no. 7, pp. 672–679, 2016.

[17] G. Messager, G. Che, H. Kasten, and C. Redemann, "Optimization of axial magnetic bearing for application of vibration assisted drilling," in *IKMT 2022; 13. GMM/ETG-Symposium*, 2022, pp. 1–6.

[18] L. Zhou and L. Li, "Modeling and identification of a solid-core active magnetic bearing including eddy currents," *IEEE/ASME Transactions on Mechatronics*, vol. 21, no. 6, pp. 2784–2792, 2016.

[19] Z. W. Whitlow, R. L. Fittro, and C. R. Knospe, "Dynamic performance of segmented active magnetic thrust bearings," *IEEE Transactions on Magnetics*, vol. 52, no. 11, pp. 1–11, 2016.

[20] R. P. Jastrzebski and O. Liukkonen, "Analysis of a segmented axial active magnetic bearing for multi-mw compressor applications," *IEEE/ASME Transactions on Mechatronics*, vol. 28, no. 5, pp. 2799–2809, 2023.

[21] J. Fu, X. Wang, L. Hou, and A. Pan, "Structure study and performance analysis on the new laminated core type axial redundant magnetic bearing," *International Journal of Applied Electromagnetics and Mechanics*, vol. 58, pp. 101–120, 2018.

[22] ClassNK, "Unified requirements for machinery installations," Aug. 2024, rev. 4. [Online]. Available: https://www.classnk.or.jp/hp/pdf/info_service/iacs_ur_and_ui/ur-m46-rev.4-aug-2024-ul.pdf

[23] L. Zhu, C. Knospe, and E. Maslen, "Analytic model for a nonlaminated cylindrical magnetic actuator including eddy currents," *IEEE Transactions on Magnetics*, vol. 41, no. 4, pp. 1248–1258, 2005.

[24] K. M. Szombati, H. Ebel, G. Ranjan, N. Nevaranta, I. F. Santos, and J. Sopanen, "Performance analysis of active magnetic bearing supported rotor system on moving platform," *SSRN Electronic Journal*, 2024, preprint available at SSRN. [Online]. Available: https://ssrn.com/abstract=5018752